Optical Engineering

OpticalEngineering.SPIEDigitalLibrary.org

High-speed high-accuracy three-dimensional shape measurement using digital binary defocusing method versus sinusoidal method

Jae-Sang Hyun
Beiwen Li
Song Zhang

SPIE.

Jae-Sang Hyun, Beiwen Li, Song Zhang, "High-speed high-accuracy three-dimensional shape measurement using digital binary defocusing method versus sinusoidal method," *Opt. Eng.* **56**(7), 074102 (2017), doi: 10.1117/1.OE.56.7.074102.

High-speed high-accuracy three-dimensional shape measurement using digital binary defocusing method versus sinusoidal method

Jae-Sang Hyun, Beiwen Li, and Song Zhang*
Purdue University, School of Mechanical Engineering, West Lafayette, Indiana, United States

Abstract. This paper presents our research findings on high-speed high-accuracy three-dimensional shape measurement using digital light processing (DLP) technologies. In particular, we compare two different sinusoidal fringe generation techniques using the DLP projection devices: direct projection of computer-generated 8-bit sinusoidal patterns (a.k.a., the sinusoidal method), and the creation of sinusoidal patterns by defocusing binary patterns (a.k.a., the binary defocusing method). This paper mainly examines their performance on high-accuracy measurement applications under precisely controlled settings. Two different projection systems were tested in this study: a commercially available inexpensive projector and the DLP development kit. Experimental results demonstrated that the binary defocusing method always outperforms the sinusoidal method if a sufficient number of phase-shifted fringe patterns can be used. [DOI: 10.1117/1.OE.56.7.074102]

Keywords: high three-dimensional optical metrology; binary defocusing method; phase-shifting algorithm; fringe analysis; structured light.

Paper 170158P received Feb. 3, 2017; accepted for publication Jun. 15, 2017; published online Jul. 6, 2017.

1 Introduction

Three-dimensional (3-D) shape measurement technologies have seen substantial growth over the past few decades and drawn significant public interest because of the commercial success of inexpensive 3-D shape measurement techniques, such as Microsoft Kinect, Intel RealSense, and Google Tango. These advancements have led to noncontact sensing or shape measurement tools for numerous applications including manufacturing, medicine, homeland security, and entertainment.[1]

The state-of-the-art 3-D shape measurement techniques have been developed to recover 3-D surface geometry at different accuracy levels based on different principles.[2] The most popular methods include the time of flight, laser triangulation, stereo vision, structured light, and digital fringe projection (DFP). All these technologies have their own merits and limitations, but no existing technology can conquer all challenges in practice; thus, no universal solution has yet come out for generic 3-D shape measurement applications. In reality, finding the most appropriate technology for a specific application is usually not easy. The handbook edited by Zhang[3] assembles a number of 3-D shape measurement techniques, making it easier for users to compare them and ultimately choose the best method for their specific application.

Time-of-flight-based 3-D shape measurement technologies (e.g., Microsoft Kinect V2) achieved great commercial success in human–computer interaction applications, where measurement accuracy is not a primary concern. For high-speed and high-accuracy applications (e.g., quality control), the structured light-based 3-D shape measurement method became one of the quickly growing technologies mainly because of its simplicity to implement, low cost, and high measurement speed.[4] Among the variations of structured light methods, the DFP technique is a special kind of structured light method in that the structured patterns vary sinusoidally and are continuous in both u- and v-directions.[2] The key difference between a DFP technique and a standard structured-light technique is that the DFP technique uses the carrier phase of sinusoidal fringe image(s) for 3-D reconstruction, whereas a standard structured light technique typically relies on the intensity of structured image(s) to find cues for 3-D shape recovery. Because the phase information is more resilient to noise, surface textural variations, ambient light conditions, etc., than the intensity, the DFP technique is overwhelmingly advantageous over other types of structured light techniques. However, using 8-bit sinusoidal patterns for the conventional DFP method has the following major limitations: (1) requirement of the nonlinear gamma correction, (2) precise synchronization requirement between the camera and the projector, and (3) existence of a speed bottleneck (typically 120 Hz).[5] To address these limitations, Lei and Zhang[6] proposed a method that uses an out-of-focus projector to project 1-bit binary patterns to approximate sinusoidal fringe patterns. Yet such a method is not trouble free, thus a thorough performance evaluation is still necessary to better understand their comparative advantages from different perspectives (e.g., phase errors, noise resistance, etc.).

This paper thus focuses on 3-D shape measurement using the DFP techniques. In particular, we analyze the differences between two different sinusoidal fringe generation mechanisms: directly projecting the 8-bit grayscale sinusoidal fringe patterns (or the sinusoidal method) versus defocusing binary patterns (or the binary defocusing method). We only focus on the use of the digital light processing (DLP) platforms for fringe generation mainly because our prior study[7]

*Address all correspondence to: Song Zhang, E-mail: szhang15@purdue.edu

0091-3286/2017/$25.00 © 2017 SPIE

found that if properly used, DLP outperforms liquid crystal on silicon–or liquid crystal display–based DFP technologies. Lei and Zhang[8] extensively examined the differences between these two technologies under different scenarios (e.g., synchronization, exposures) when a commercial DLP projector is used, and a three-step phase-shifting algorithm is used for high-speed applications; Zhang et al.[9] and Li et al.[5] have demonstrated the speed advantages using the binary defocusing method over the sinusoidal method, and Li and Zhang[10] examined the differences between these two technologies under a microscale using a telecentric lens. Instead of repeating all prior studies, this paper builds upon our prior findings and mainly evaluates the performance differences for high-accuracy measurement applications under precisely controlled settings (e.g., synchronization control and nonlinear gamma compensation). We examine two different projection systems in this study: the commercially available inexpensive projector (model: Dell M115HD) and the DLP development kit (model: DLP Lightcrafter 4500). This paper explains the principle behind each method and compares simulation and experimental data to demonstrate their differences.

Section 2 discusses the basics of the DLP technology, the phase-shifting algorithm, and two types of sinusoidal fringe generation methods. Section 3 shows simulation results. Section 4 presents experimental results. Section 5 discusses our findings from this research as well as our prior studies; finally, Sec. 6 summarizes this paper.

2 Principle

2.1 *Fundamentals of Digital Light Processing Technology*

The DLP projector produces grayscale values of a pixel by properly tilting the micromirror of the digital micromirror device (DMD) either into or away from the optical path rapidly with a proper timing ratio.[11] Figure 1 shows the experimental data of the timing signal under different grayscale values for a commercial DLP projector. These experiments used a photodiode to sense the output light of the DLP projector; the sensed current signal was then converted to voltage by a resistor, and the converted voltage signal is monitored by an oscilloscope. For all these experiments, only a full-screen green image was used to better visualize the effect. Figure 1(a) shows that when the projector is fed with a full-range green image (i.e., green = 255), the DMD stays in the ON state for almost 100% of the time. Figures 1(b) and 1(c) show irregular waveforms when the grayscale value reduces to 128 and 64, respectively. It shows ~50% ON time when green = 128, and ~25% ON time when green = 64. If the grayscale value is reduced to 0, the DMD stays in the OFF state all the time, or 0% ON time, as shown in Fig. 1(d). These simple experiments indicate that the full projection cycle must be used to properly capture an 8-bit sinusoidal grayscale pattern because a sinusoidal pattern's grayscale value ranges from 0 to 255. In contrast, a binary pattern only uses two grayscale values (0 and 255); thus, a partial projection cycle is sufficient to represent the pattern, that is, one can use an illumination time shorter than the projection cycle to capture the projected binary pattern without any problems.

2.2 *Phase-Shifting Algorithm*

Phase-shifting algorithms have been extensively employed in optical metrology because of their speed, accuracy, and robustness to noise.[12] In history, numerous phase-shifting algorithms have been developed, with some being faster and some being more robust. In general, for an N-step phase-shifting algorithm with equal phase shifts, the k'th fringe pattern can be mathematically described as

$$I_k(x,y) = I'(x,y) + I''(x,y)\cos(\phi + 2k\pi/N), \tag{1}$$

where $I'(x,y)$ is the average intensity, $I''(x,y)$ is the intensity modulation, $\phi(x,y)$ is the phase to be solved for, and $k = 1, 2, \ldots, N$. The phase $\phi(x,y)$ can be calculated by simultaneously solving these equations,

$$\phi(x,y) = -\tan^{-1}\frac{\sum_{k=1}^{N} I_k(x,y)\sin(2k\pi/N)}{\sum_{k=1}^{N} I_k(x,y)\cos(2k\pi/N)}. \tag{2}$$

Due to the use of an arctangent function, the phase obtained from Eq. (2) ranges from $-\pi$ to π with a modulus of 2π. The phase is also called the wrapped phase. To recover the real continuous phase, a phase unwrapping algorithm has to be employed. Phase unwrapping essentially detects and removes 2π discontinuities by adding or subtracting integer multiples of 2π. In general, the phase unwrapping algorithm can be classified into two categories: spatial phase unwrapping and temporal phase unwrapping. The spatial phase unwrapping[13] typically gives relative phase information because the unwrapped phase is relative to a point on the phase map. To recover the 3-D shape, the spatially unwrapped phase map typically uses a reference-plane-based method. The temporal phase unwrapping, in contrast, recovers absolute phase by acquiring additional images. Once the absolute phase is known, and the geometry of the system is properly calibrated, then the absolute (x, y, z)

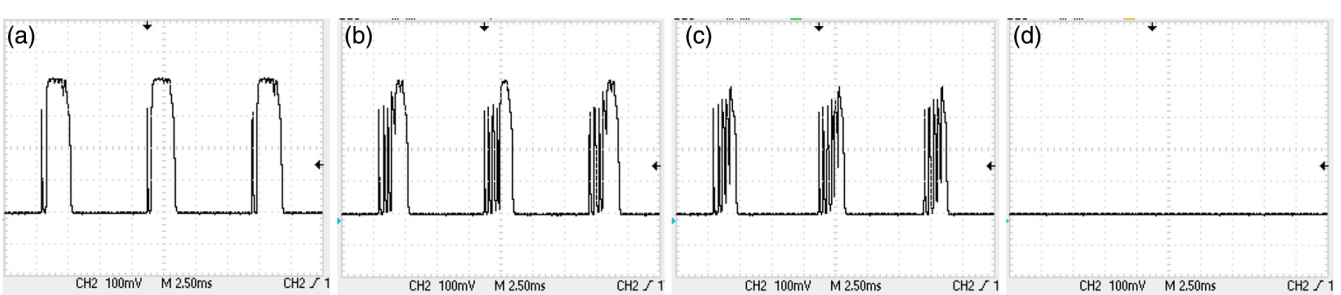

Fig. 1 Example of the DLP projector's timing signal with different intensity of green light (red = blue = 0). (a) Green = 255, (b) green = 128, (c) green = 64, and (d) green = 0.

coordinates can be reconstructed from the absolute phase.[14] In this research, we employ the temporal phase unwrapping (i.e., the gray-coding method) to unwrap the phase pixel by pixel.

2.3 *Sinusoidal Fringe Pattern Generation*

There are two ways of generating sinusoidal fringe patterns: directly projecting the computer-generated 8-bit grayscale sinusoidal fringe patterns (i.e., the sinusoidal method) and defocusing the binary patterns (i.e., the binary defocusing method). The former is straightforward. For example, assuming the sinusoidal fringe pattern varies along the i-direction, the discrete version of the fringe pattern shown in Eq. (1) can be created by a computer as

$$I_k^c(i,j)=(G_{\max}-G_{\min})[0.5+0.5\cos(2\pi i/T+2k\pi/N)]+G_{\min}, \tag{3}$$

where (i, j) is the pixel coordinate on the projector, T is fringe pitch, i.e., the number of pixels per fringe period, and $G_{\max}$ and $G_{\min}$ are the maximum and minimum grayscale values one can use. Typically $G_{\max} < 255$ and $G_{\min} > 0$. If the projector is a linear device, this pattern can be directly projected for phase retrieval.

The second approach of generating sinusoidal patterns is using the binary defocusing method.[6] The most straightforward method of generating a sinusoidal pattern is to change the focus of the projector to deform a square binary pattern to a pseudo sinusoidal pattern. For example, the same sinusoidal fringe pattern shown in Eq. (4) can be created by properly defocusing the square binary pattern created by a computer as

$$I_k^b(i,j) = 255\left\{\text{floor}\left[\frac{i+k\times T/N+3T/4 \bmod T)}{T/2}\right]\right\}, \tag{4}$$

where floor() is an operator that truncates the decimals of a floating point value to an integer number, and mod is the modulus operator.

Over history, researchers have developed optimization algorithms to improve the quality of binarized grayscale images[15–21] or to improve the quality of phase.[22–31] Our experience found that for narrow fringe patterns (i.e., fringe period <18 pixels), even if a three-step phase-shifting algorithm is adopted, using standard square binary patterns is better than using any of those optimized patterns; if the fringe pattern is very wide (e.g., fringe period >120 pixels), a standard error-diffusion dithering technique works reasonably well for high-quality measurement. Therefore, the optimization approaches are typically valuable if fringe periods are in the middle range [e.g., fringe pitch $T \in (18, 120)$ pixels].

2.4 *Projector Nonlinear Gamma Correction*

As 3-D coordinates are directly recovered from the phase using the calibrated system parameters, the phase quality ultimately determines the measurement quality: any noise or error on the phase will be directly mapped to the final 3-D measurement result. Because the sinusoidal method requires the use of a full grayscale range (i.e., from 0 to 255), the nonlinearity of the DFP system is required to be properly calibrated and corrected to ensure high-quality measurement. The dominant nonlinear effect of the DFP system is actually the nonlinear response of the commercial projector that is designed to compensate for the human visual perception system. This nonlinear response is often referred to as the gamma response because the curve is close to an exponential function (i.e., $y = a + bx^{\gamma}$, where a, b, and gamma are constants). Even though nonlinearity calibration is relatively mature with many developed methods,[32–37] our research[1] found that the nonlinearity of the projector actually changes over time, complicating this type of problem as a nonlinear gamma calibration has to be performed regularly. Nevertheless, good-quality phase can be obtained by properly calibrating the nonlinear gamma shortly before measurement and applying a proper nonlinear gamma correction algorithm. In this paper, we use the active gamma calibration method that we developed for nonlinear gamma correction.[38]

2.5 *High-Frequency Harmonics Reduction*

The binary defocusing method is not affected by the nonlinear gamma of the projector, yet the pattern generated by this method is not ideally sinusoidal. The lens defocusing essentially suppresses high-frequency harmonics yet preserves the fundamental frequency. However, the high-frequency harmonics will not be completely eliminated in theory, and ideal sinusoidal fringe patterns still cannot be created after lens defocusing. Due to the nature of phase-shifting algorithms, especially with equal phase shifts, the high-frequency harmonic error can be naturally eliminated if the proper number of phase shift steps (N) is used. If the phase shift step number N is the same as the fringe period (i.e., $T = N$), the harmonics do not introduce any phase error.[39] Therefore, if fringe patterns are narrow, it is preferable to use the proper number of phase shift steps to fundamentally eliminate the error caused by high-frequency harmonics.

As mentioned above, if fringe patterns are wide, an error-diffusion algorithm[20,21] should be able to provide sufficiently high-quality fringe patterns. If one tends to use middle-range fringe patterns, one of the optimization approaches[22–31] can be employed to improve the phase quality. As for high-quality measurement, narrow fringe patterns are preferable; this study will compare the performance of standard square binary patterns with sinusoidal fringe patterns with the use of a proper number of phase-shifted fringe patterns.

3 Simulation

Figure 2 shows the simulation results of the performance differences between these two fringe pattern generation methods. We chose different phase shift numbers, such as $N = 10$, 18, 26, and 34 that are the same as fringe pitches, $T = N$. We added zero-mean Gaussian noise with a standard deviation of 0.1 for normalized fringe patterns (or 10% noise). For all these simulations, we applied no smoothing filters to emulate the perfectly focused hardware system setups. As one can clearly see, without averaging, the phase root-mean-square (rms) error from the phase-shifted binary patterns is approximately half of that from the phase-shifted sinusoidal patterns. It is well known that the averaging effect can reduce the random noise and improve the signal-to-noise ratio (SNR). These figures also include phase rms errors after different levels of averaging. As one can see, if the averaging is applied for five or more times, the difference between the

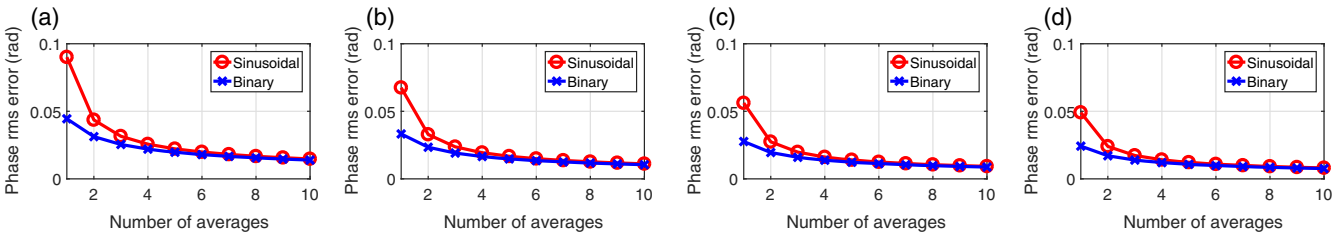

Fig. 2 Simulation results of different fringe periods with different number of averaging. (a) Fringe pitch $T = 10$ pixels, (b) fringe pitch $T = 18$ pixels, (c) fringe pitch $T = 26$ pixels, and (d) fringe pitch $T = 34$ pixels.

binary defocusing method and the sinusoidal method is not obvious for all fringe periods.

In summary, these simulation results indicate that (1) for $N = T$ step phase-shifting algorithm, the harmonics impact of the square binary patterns is completely eliminated; (2) without averaging, using binary patterns is much better than directly using sinusoidal patterns; (3) sufficient averaging makes the difference between these two methods negligible. Therefore, overall, our simulation suggests the binary defocusing method works better for low SNR conditions, and that both methods work equally well for high SNR conditions, albeit the binary defocusing method works slightly better.

4 Experiment

We set up two systems with the same camera but different projectors to experimentally demonstrate the differences between these two types of fringe generation methods. Figure 3 shows the photographs of these two systems. For both systems, we used a CCD camera (model: the Imaging Source DMK 23U618) that is attached with a 12-mm focal length lens (model: Computar M1214-MP2). The camera resolution was set as 640×480 pixels. The first system (the Dell projector system) used a commercially available LED projector (model: Dell M115HD), and the projector's native resolution is 1280×800 pixels; and the second system (the Lightcrafter system) used a DLP development kit (model: DLP Lightcrafter 4500), which has a 912×1140 pixels natural resolution.

For both systems, the camera's exposure time was set as $1/60$ s to fairly compare these two fringe generation methods as the Dell projector refreshes at 60 Hz, and the sinusoidal pattern should be correctly captured by choosing an exposure time that is the same as the refreshing period. The Dell projector was synchronized with the camera through VGA's VSync signal, and the Lightcrafter projector was synchronized with the camera using an external microprocessor (model: Arduino UNO) that simultaneously sends two trigger signals: one to the camera and one to the projector. The Lightcrafter was setup with an exposure time of $1/60$ s as well for both sinusoidal and binary methods.

For all experiments, the projector was only slightly defocused to eliminate the pixelate effect, and only the green channel of the projector was turned on. The nonlinear gamma for the Dell projector was calibrated and compensated for by the active calibration method we developed.[36] As the Lightcrafter is a linear device, no gamma calibration is necessary for sinusoidal pattern generation.

For both systems, a flat white paper was measured to characterize their performance. We captured phase-shifted fringe patterns with steps $N = 10$, 18, 26, and 34 and fringe periods $T = N$ pixels. Each fringe pattern was captured 10 times for both sinusoidal and binary methods at two different intensity values: the bright case represents the well-exposed situation with a high SNR, whereas the dark case represents a larger noise impact with a lower SNR. Figure 4 shows one representative fringe pattern with a fringe period of 26 pixels for two different SNR conditions. One can see that the projector is well focused for both the sinusoidal method and binary defocusing method.

We compared the measured phase quality by taking the difference between the measured phase Φ and a reference phase Φ^r. The reference map was generated by taking 20 averages of $N = 18$ phase-shifted fringe patterns with a fringe period of $T = 18$ pixels, and then smoothed out by a Gaussian filter with a size of 21×21 pixels. To compute phase error, we took the difference between the measured phase map Φ with a fringe period of T pixels and the reference phase map Φ^r with a fringe period of 18 pixels as

$$\Delta\Phi = \Phi - \Phi^r \times T/18. \tag{5}$$

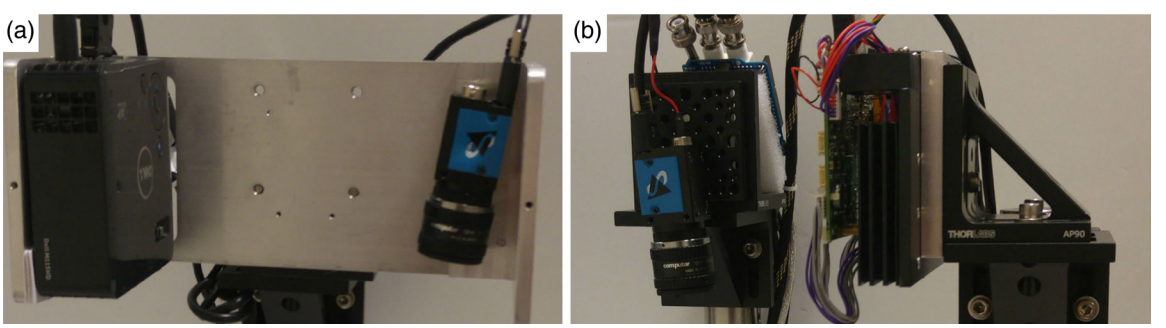

Fig. 3 Experimental setup. (a) The Dell projector system and (b) the Lightcrafter projector system.

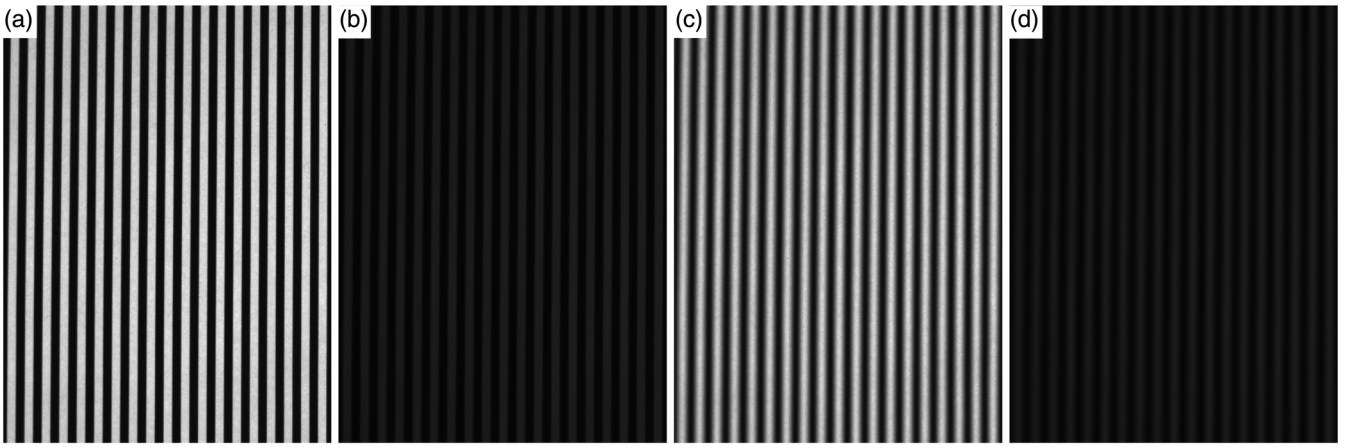

Fig. 4 Example fringe images with high and low SNRs for fringe period $T = 26$ captured by the Lightcrafter projector system. (a) High SNR (bright) binary pattern, (b) low SNR (dark) binary pattern, (c) high SNR (bright) sinusoidal pattern, and (d) low SNR (dark) sinusoidal pattern.

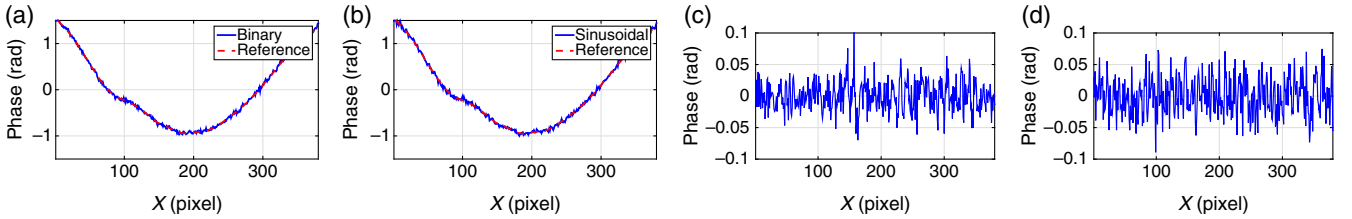

Fig. 5 Cross sections of the reference phase and the measured phase for the Dell projector system. (a) Cross sections of these phase maps for the binary defocusing method, (b) cross sections of these phase maps for the sinusoidal method, (c) cross section of the difference phase map for the binary defocusing method (rms error: 0.023 rad), and (d) cross section of the difference phase map for the sinusoidal method (rms error: 0.029 rad).

Figures 5(a), 5(b) and 6(a), 6(b) show the same cross sections of the reference plane phase and the measured plane phase after removing gross slope when $T = 10$ pixels. Clearly, the reference plane phase Φ_r only represents the shape of the uniform white flat board, thus it can be subtracted from the phase data to characterize the measurement error. For the Dell projector system, as shown in Figs. 5(c) and 5(d), the rms error for the binary defocusing method is ~0.023 rad, and for the sinusoidal method, it is ~0.029 rad; for the Lightcrafter projector system, the rms errors are ~0.022 and 0.029 rad as shown in Figs. 6(c) and 6(d), respectively.

We first analyzed the lower SNR condition with different numbers of averaging, and Fig. 7 shows the comparative results. These results show that before any averaging, the binary defocusing method clearly outperforms the sinusoidal method for all fringe periods. If a few times averages are used, the differences become smaller, yet the binary defocusing method is still slightly better than the sinusoidal method.

We then analyzed the high SNR cases, and Fig. 8 shows the results. One may notice that compared with the lower SNR cases shown in Fig. 7, the averaging only slightly affects the high SNR cases. This is because for high SNR cases, the random noise is very small, and the data without averaging are already of high quality. One may also notice that for all high SNR cases, the binary defocusing method is consistently better than the sinusoidal method. All these experimental data are consistent with our simulation results, confirming that the binary defocusing method indeed outperforms the sinusoidal method if sufficient numbers of phase-shifted fringe patterns can be used.

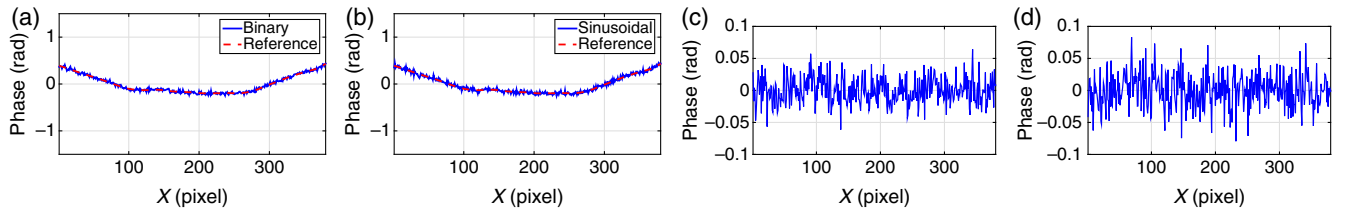

Fig. 6 Cross sections of the reference phase and the measured phase for the Lightcrafter projector system. (a) Cross sections of these phase maps for the binary defocusing method, (b) cross sections of these phase maps for the sinusoidal method, (c) cross section of the difference phase map for the binary defocusing method (rms error: 0.022 rad), and (d) cross section of the difference phase map for the sinusoidal method (rms error: 0.029 rad).

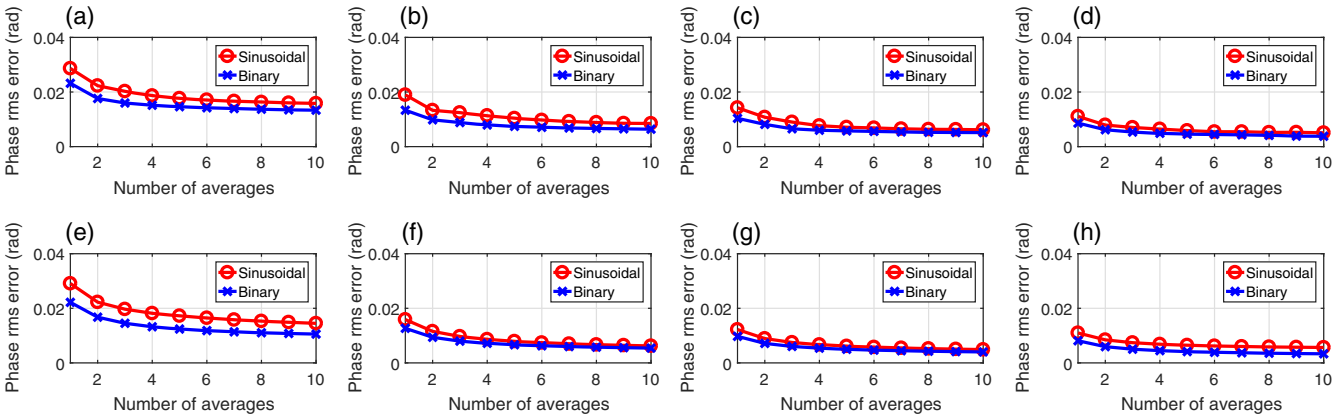

Fig. 7 Experimental results of different fringe periods with different number of averaging for the low SNR case. The first row shows the results captured by the Dell projector system, and the second row shows the results captured by the Lightcrafter system. (a) Fringe pitch $T = 10$ pixels, (b) fringe pitch $T = 18$ pixels, (c) fringe pitch $T = 26$ pixels, (d) fringe pitch $T = 34$ pixels, (e) fringe pitch $T = 10$ pixels, (f) fringe pitch $T = 18$ pixels, (g) fringe pitch $T = 26$ pixels, and (h) fringe pitch $T = 34$ pixels.

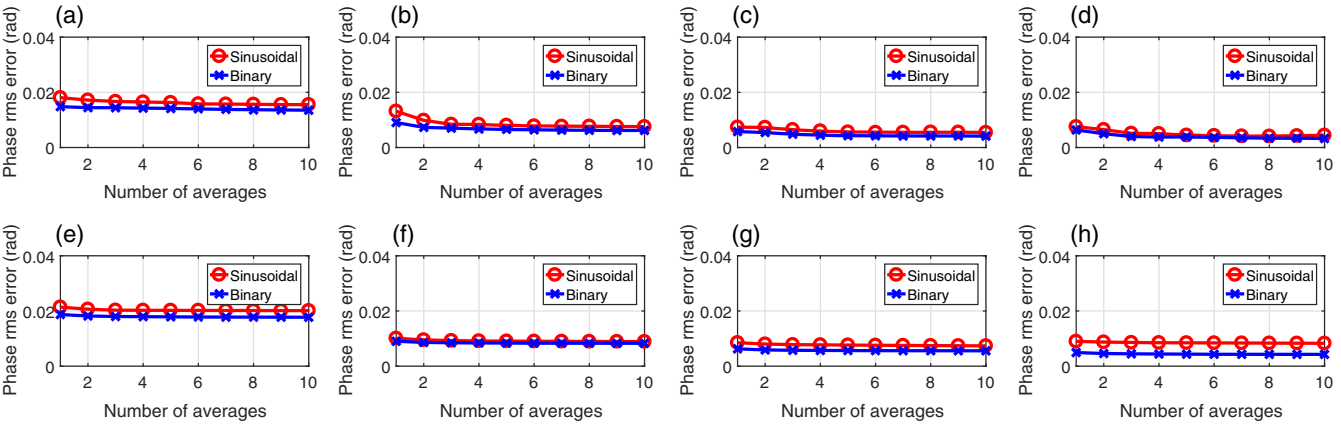

Fig. 8 Experimental results of different fringe periods with different number of averaging for the high SNR case. The first row shows the results captured by the Dell projector system, and the second row shows the results captured by the Lightcrafter system. (a) Fringe pitch $T = 10$ pixels, (b) fringe pitch $T = 18$ pixels, (c) fringe pitch $T = 26$ pixels, (d) fringe pitch $T = 34$ pixels, (e) fringe pitch $T = 10$ pixels, (f) fringe pitch $T = 18$ pixels, (g) fringe pitch $T = 26$ pixels, and (h) fringe pitch $T = 34$ pixels.

5 Discussion

Lei and Zhang[8] thoroughly compared the performance of the binary defocusing method and the sinusoidal method, and the major findings were as follows:

- No gamma correction is required for the binary defocusing method: The sinusoidal method is very sensitive to the projector's nonlinear gamma effect; thus, the gamma calibration is mandatory for a commercial digital video projector. In contrast, the binary defocusing method is not sensitive to the projector gamma because only two grayscale levels are used.
- Synchronization between the projector and the camera is more relaxed for the binary defocusing method: For the sinusoidal method, because more than two grayscale values are used, the camera and the projector must be precisely synchronized for high-quality 3-D shape measurement. In contrast, for the binary defocusing method, because the sinusoidal fringe patterns are generated by defocusing binary patterns, the synchronization is less important.
- It is more difficult for the binary defocusing method to achieve high accuracy if a three-step phase-shifting algorithm is used: Because the sinusoidal patterns are not generated directly by the computer, the degree of defocusing affects the measurement quality. In contrast, as the sinusoidal method can use an infocused projector, it is not affected by the amount of defocusing.
- Smaller depth measurement range can be achieved for the binary defocusing method if a three-step phase-shifting algorithm is used. For the binary defocusing method, the projector must be properly defocused to generate good-quality sinusoidal fringe patterns; otherwise, the nonsinusoidal waveform will cause a large error. In contrast, the sinusoidal method is not very sensitive to this problem because the degree of defocusing will not affect the fringe profile.

Li and Zhang[10] compared these two sinusoidal fringe generation methods through simulation and experiments under microscopic systems. Two types of microscopy systems were tested: (1) both camera and projector use telecentric lenses and (2) only the camera uses a telecentric lens.

- Simulation demonstrated that the binary defocusing method outperforms the sinusoidal method for an N-step phase-shifting algorithm ($N = 18$ and $T = 18$ pixels). If the signal has a zero-mean Gaussian noise with a standard deviation of 5% of signal intensity, the phase rms error from the sinusoidal method almost doubles that from the binary defocusing method for the N-step phase-shifting algorithm without averaging. The averaging could reduce the gap, but the binary defocusing method is still slightly better.
- Experimental data confirmed the simulation results for both types of systems. For a practical measurement system, depth resolution can be improved by ~19% using the binary defocusing method instead of the sinusoidal method.

The major findings of this research through simulation and experiments are summarized as follows:

- The findings of this paper are consistent with what Li and Zhang[10] have found in the paper for macrorange 3-D shape measurement systems: the binary defocusing method has a much better performance than the sinusoidal method when $N = T$ (N is the step of the equal phase shifts and T is the fringe period) for all cases ($N = T = 10$, 18, 26, and 34) we used in this research.
- For both high SNR and low SNR cases, the binary defocusing method consistently outperforms the sinusoidal method. For the low SNR case, the image averaging can slightly reduce the difference between these two methods; yet for the high SNR case, the image averaging does not have an obvious impact.

Furthermore, the speed benefit of using the binary defocusing method is apparent, especially if one uses the DLP development kit. For example, the DLP Lightcrafter 4500 projector we used for this study can switch binary patterns at 4225 Hz, whereas it only switches 8-bit grayscale images at 120 Hz. This study as well as our previous studies found that the binary defocusing method not only leads to speed breakthroughs for 3-D shape measurement but also can improve measurement quality. Therefore, it seems that one should use the binary defocusing method over the traditional sinusoidal method for both high-speed and high-accuracy measurements provided that the proper phase-shifting method can be selected.

6 Summary

This paper has compared the performance of two sinusoidal fringe pattern generation methods: binary defocusing and direct sinusoidal fringe projection. Due to the use of phase-shifting, we found that if a sufficient number of phase-shifted fringe patterns is used, and the projector is slightly defocused to remove the pixelate effect, the phase quality generated from the binary defocusing method is actually higher than that from the sinusoidal method for the commercially available DLP projector and for the DLP development kit. And if sufficient averaging is allowed for random noise reduction, both methods generate similar quality phase, albeit using binary patterns is still slightly better. These findings are consistent with our prior study[10] from both simulation and experiments for microscopic systems. Therefore, in general, it seems that one should use the binary defocusing method over the traditional sinusoidal method for both high-speed and high-accuracy measurements provided that the proper phase-shifting method can be selected.

Acknowledgments

The work presented in this paper was carried out by numerous collaborators and the authors would like to thank all of them. This study was sponsored by the National Science Foundation (NSF) under grant numbers: CMMI-1531048 and CMMI-1523048. The views expressed in this paper are those of the authors and not necessarily those of the NSF.

References

1. S. Zhang, "Recent progresses on real-time 3-D shape measurement using digital fringe projection techniques," *Opt. Lasers Eng.* **48**(2), 149–158 (2010).
2. B. Li et al., "High-accuracy, high-speed 3D structured light imaging techniques and potential applications to intelligent robotics," *Int. J. Intell. Rob. Appl.* **1**(1), 86–103 (2017).
3. S. Zhang, Ed., *Handbook of 3D Machine Vision: Optical Metrology and Imaging*, 1st ed., CRC Press, New York (2013).
4. J. Geng, "Structured-light 3D surface imaging: a tutorial," *Adv. Opt. Photonics* **3**(2), 128–160 (2011).
5. B. Li et al., "Some recent advances on superfast 3D shape measurement with digital binary defocusing techniques," *Opt. Lasers Eng.* **54**, 236–246 (2014).
6. S. Lei and S. Zhang, "Flexible 3-D shape measurement using projector defocusing," *Opt. Lett.* **34**(20), 3080–3082 (2009).
7. S. Zhang, *High-Speed 3D Imaging with Digital Fringe Projection Technique*, 1st ed., CRC Press, New York (2016).
8. S. Lei and S. Zhang, "Digital sinusoidal fringe generation: defocusing binary patterns VS focusing sinusoidal patterns," *Opt. Lasers Eng.* **48**(5), 561–569 (2010).
9. S. Zhang, D. van der Weide, and J. Oliver, "Superfast phase-shifting method for 3-D shape measurement," *Opt. Express* **18**(9), 9684–9689 (2010).
10. B. Li and S. Zhang, "Microscopic structured light 3D profilometry: binary defocusing technique VS sinusoidal fringe projection," *Opt. Lasers Eng.* **96**, 117–123 (2017).
11. L. J. Hornbeck, "Digital light processing for high-brightness, high-resolution applications," *Proc. SPIE* **3013**, 27–40 (1997).
12. D. Malacara, Ed., *Optical Shop Testing*, 3rd ed., John Wiley and Sons, New York (2007).
13. D. C. Ghiglia and M. D. Pritt, Eds., *Two-Dimensional Phase Unwrapping: Theory, Algorithms, and Software*, John Wiley and Sons, New York (1998).
14. S. Zhang and P. S. Huang, "Novel method for structured light system calibration," *Opt. Eng.* **45**, 083601 (2006).
15. W. Purgathofer, R. Tobler, and M. Geiler, "Forced random dithering: improved threshold matrices for ordered dithering," in *Proc. IEEE Int. Conf. Image Processing (ICIP 1994)*, Vol. 2, pp. 1032–1035 (1994).
16. T. D. Kite, B. L. Evans, and A. C. Bovik, "Modeling and quality assessment of halftoning by error diffusion," *IEEE Trans. Image Process.* **9**(5), 909–922 (2000).
17. T. Xian and X. Su, "Area modulation grating for sinusoidal structure illumination on phase-measuring profilometry," *Appl. Opt.* **40**(8), 1201–1206 (2001).
18. T. L. Schuchman, "Dither signals and their effect on quantization noise," *IEEE Trans. Commun.* **12**(4), 162–165 (1964).
19. B. Bayer, "An optimum method for two-level rendition of continuous-tone pictures," in *IEEE Int. Conf. on Communications*, Vol. 1, pp. 11–15 (1973).
20. R. Floyd and L. Steinberg, "An adaptive algorithm for spatial gray scale," in *Proc. Society for Information Display*, Vol. 17, pp. 75–77 (1976).
21. P. Stucki, "Mecca: a multiple-error correcting computation algorithm for bilevel hardcopy reproduction," Technical Report, IBM Research Laboratory, Zurich, Switzerland (1981).
22. C. Zuo et al., "Optimized pulse width modulation pattern strategy for three-dimensional profilometry with projector defocusing," *Appl. Opt.* **51**(19), 4477–4490 (2012).

23. T. Yoshizawa and H. Fujita, "Liquid crystal grating for profilometry using structured light," *Proc. SPIE* **6000**, 60000H (2005).
24. H. Fujita et al., "Three-dimensional profilometry using liquid crystal grating," *Proc. SPIE* **5058**, 51 (2003).
25. G. A. Ayubi et al., "Pulse-width modulation in defocused 3-D fringe projection," *Opt. Lett.* **35**, 3682–3684 (2010).
26. W. Lohry and S. Zhang, "Genetic method to optimize binary dithering technique for high-quality fringe generation," *Opt. Lett.* **38**(4), 540–542 (2013).
27. J. Dai, B. Li, and S. Zhang, "High-quality fringe patterns generation using binary pattern optimization through symmetry and periodicity," *Opt. Lasers Eng.* **52**, 195–200 (2014).
28. J. Sun et al., "Improved intensity-optimized dithering technique for 3D shape measurement," *Opt. Lasers Eng.* **66**, 158–164 (2015).
29. Y. Wang and S. Zhang, "Optimum pulse width modulation for sinusoidal fringe generation with projector defocusing," *Opt. Lett.* **35**(24), 4121–4123 (2010).
30. W. Lohry and S. Zhang, "Fourier transform profilometry using a binary area modulation technique," *Opt. Eng.* **51**(11), 113602 (2012).
31. W. Lohry and S. Zhang, "3D shape measurement with 2D area modulated binary patterns," *Opt. Lasers Eng.* **50**(7), 917–921 (2012).
32. S. Kakunai, T. Sakamoto, and K. Iwata, "Profile measurement taken with liquid-crystal grating," *Appl. Opt.* **38**(13), 2824–2828 (1999).
33. H. Guo, H. He, and M. Chen, "Gamma correction for digital fringe projection profilometry," *Appl. Opt.* **43**, 2906–2914 (2004).
34. B. Pan et al., "Phase error analysis and compensation for nonsinusoidal waveforms in phase-shifting digital fringe projection profilometry," *Opt. Lett.* **34**(4), 416–418 (2009).
35. P. S. Huang, C. Zhang, and F.-P. Chiang, "High-speed 3-D shape measurement based on digital fringe projection," *Opt. Eng.* **42**(1), 163–168 (2003).
36. S. Zhang and P. S. Huang, "Phase error compensation for a three-dimensional shape measurement system based on the phase shifting method," *Opt. Eng.* **46**(6), 063601 (2007).
37. S. Zhang and S.-T. Yau, "Generic nonsinusoidal phase error correction for three-dimensional shape measurement using a digital video projector," *Appl. Opt.* **46**(1), 36–43 (2007).
38. S. Zhang, "Comparative study on passive and active projector nonlinear gamma calibration," *Appl. Opt.* **54**(13), 3834–3841 (2015).
39. B. Chen and S. Zhang, "High-quality 3D shape measurement using saturated fringe patterns," *Opt. Lasers Eng.* **87**, 83–89 (2016).

Jae-Sang Hyun is a PhD student working with Dr. Song Zhang in the School of Mechanical Engineering at Purdue University. His research interests are three-dimensional optical metrology, robotics, and embedded systems.

Beiwen Li is a PhD candidate working with Dr. Song Zhang in the School of Mechanical Engineering at Purdue University. He received his master's degree from Iowa State University in 2014. His research interests are superfast (kHz) 3-D imaging, multiscale 3-D optical metrology, machine vision, online inspection, and mechanics analysis.

Song Zhang received his PhD from Stony Brook University in 2005. He is an associate professor in mechanical engineering, Purdue University, Indiana. His current research interests include 3-D machine/computer vision, biophotonic imaging, virtual reality, augment vision, human computer interactions, forensic science, and biomedical engineering. He has authored or coauthored over 100 research articles. He is the recipient of a NSF CAREER award in 2012 and a fellow of SPIE.